

This item is the archived peer-reviewed author-version of:

Role of coating-metallic support interaction in the properties of electrosynthesized Rh-based structured catalysts

Reference:

Benito Patricia, de Nolf Wout, Nuyts Gert, Janssens Koen, et al.- Role of coating-metallic support interaction in the properties of electrosynthesized Rh-based structured catalysts

ACS catalysis - ISSN 2155-5435 - 4:10(2014), p. 3779-3790

Full text (Publishers DOI): <http://dx.doi.org/doi:10.1021/cs501079k>

To cite this reference: <http://hdl.handle.net/10067/1222150151162165141>

Role of Coating-Metallic Support Interaction in the Properties of Electrosynthesized Rh-Based Structured Catalysts

Patricia Benito^{†*}, Wout de Nolf^{‡**}, Gert Nuyts[‡], Marco Monti[†], Giuseppe Fornasari[†],
Francesco Basile[†], Koen Janssens[‡], Francesca Ospitali[†], Erika Scavetta[†], Domenica Tonelli[†],
Angelo Vaccari[†]

[†] Dipartimento di Chimica Industriale “Toso Montanari”, ALMA MATER STUDIORUM -
Università di Bologna, Viale Risorgimento 4, 40136, Bologna, Italy

[‡] Department of Chemistry, University of Antwerp, Groenenborgerlaan 171, 2020 Antwerp,
Belgium

corresponding authors: *patricia.benito3@unibo.it; **wout.denolf@uantwerpen.be

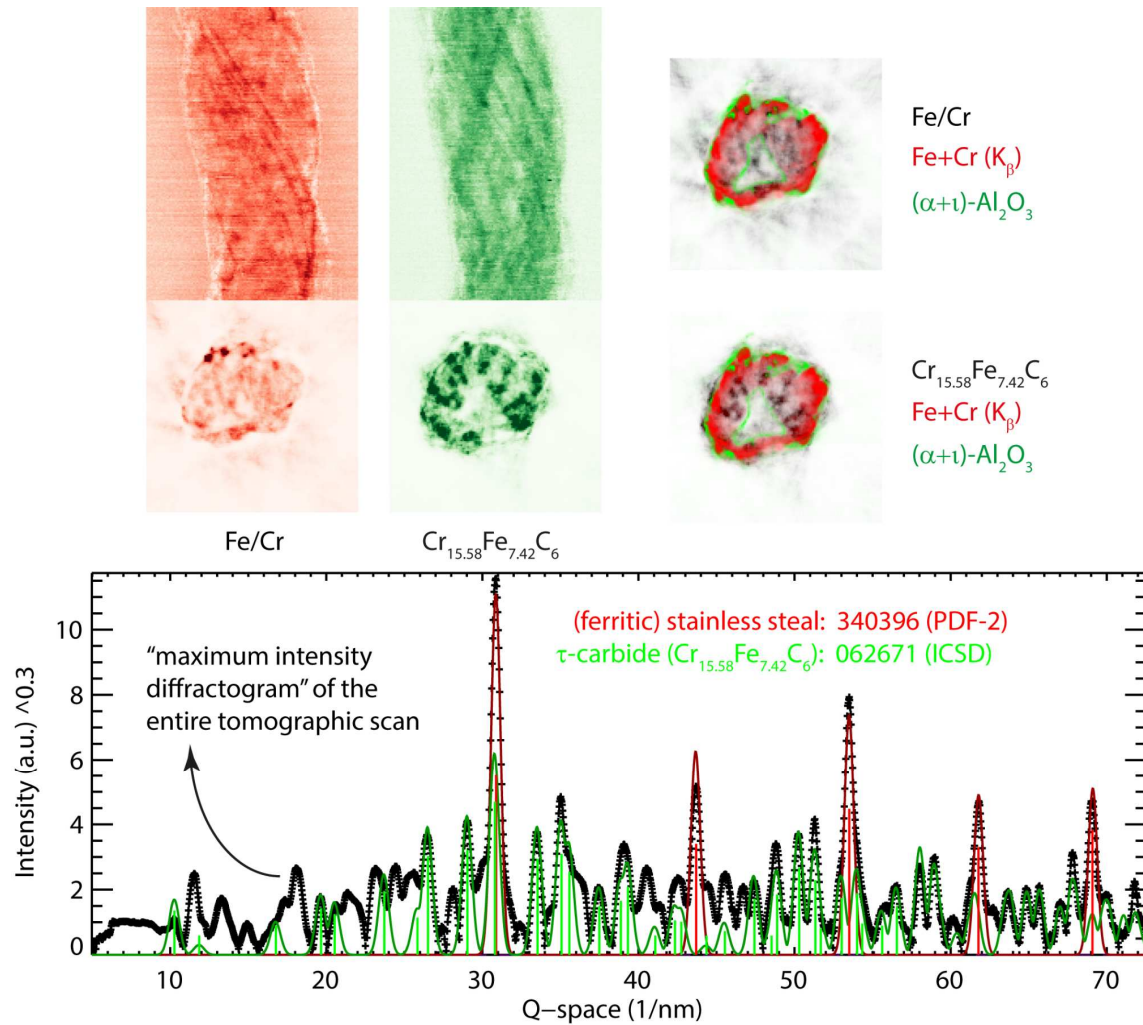


Figure S1. Reconstructions of the Fe/Cr alloy bulk material (stainless steel with ferrite crystal structure) and τ -carbide ($\text{Cr}_{23+x}\text{Fe}_x\text{C}_6$ with $x = 7.42$) in a $\text{Rh}_{11.0}\text{Mg}_{70.0}\text{Al}_{19.0}$ strut (state C). Translation: $170 \mu\text{m}$ ($1.3 \mu\text{m}$ steps); Rotation: 180° (1° steps); Time: 1 s per point. Comparison with the Fe+Cr elemental distribution and the alumina scale (both defining the inner and outer surface of the foam) shows that the reconstruction of Fe/Cr and τ -carbide is unreliable. The sinograms are obtained by fitting all diffractograms with a model that includes the τ -carbide (ICSD 062671) and ferrite (AMCSD 0011214) crystal structures, as illustrated for the "maximum intensity diffractogram" of the entire tomographic scan.

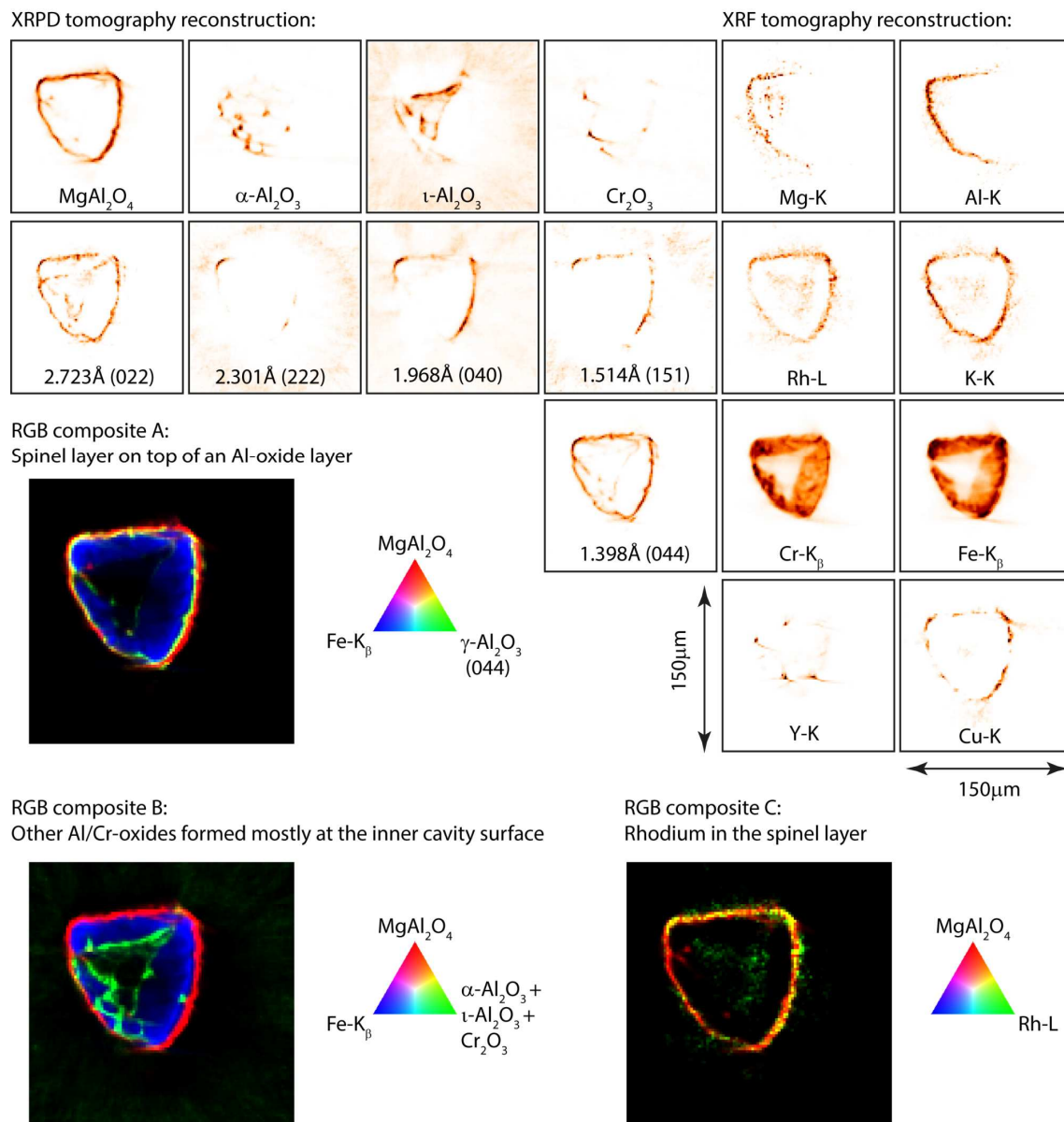


Figure S2. Elemental and crystalline distributions in a virtual cross-section of a calcined Rh_{5.0}Mg_{70.0}Al_{25.0} strut (state C). Translation: 150 μm (1.5 μm steps); Rotation: 180° (1.2° steps); Time: 1 s per point. The unidentified reflections may be attributed to γ -Al₂O₃. RGB composite maps show that roughly two layers are formed on top of the foam surface: a spinel layer (containing rhodium) and an oxide layer which takes the form of γ -Al₂O₃ at the outer foam surface and α / τ -Al₂O₃/Cr₂O₃ at the inner cavity surface.

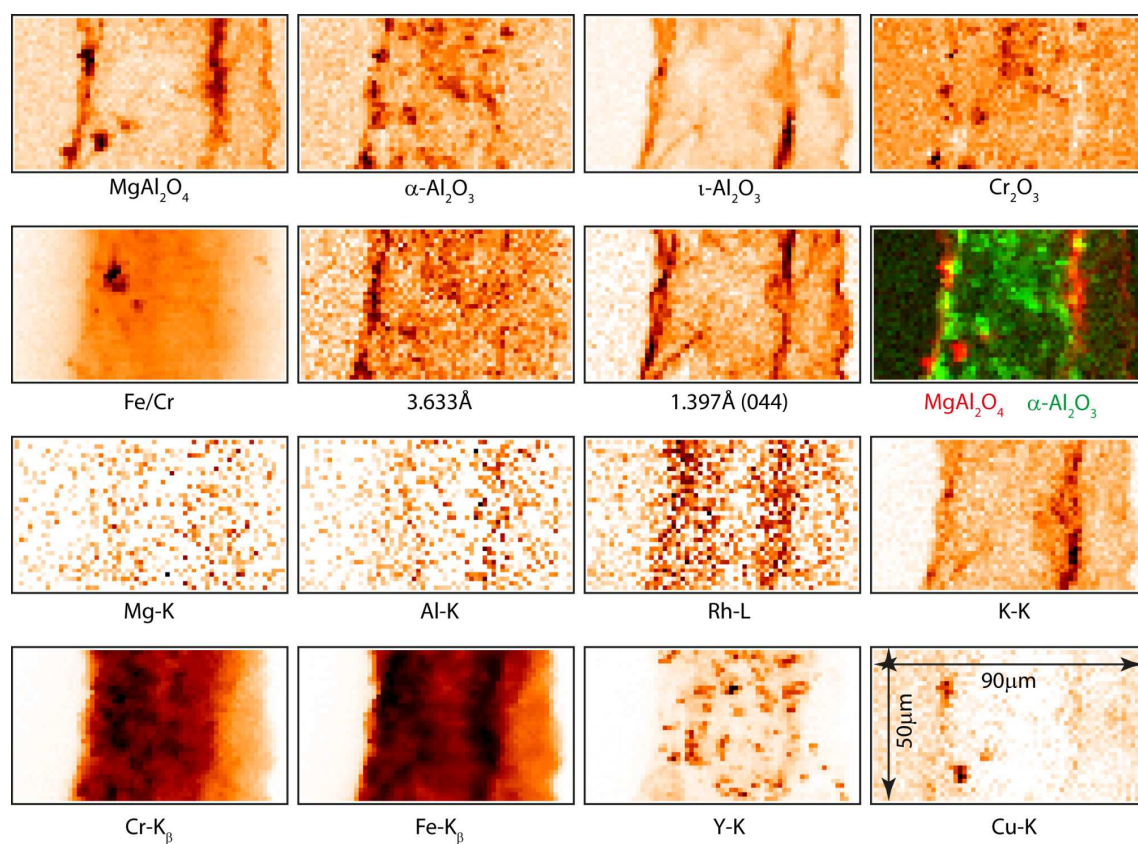
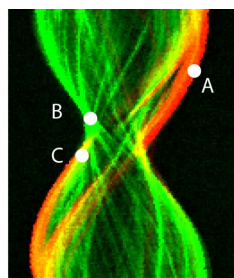
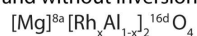


Figure S3. Projected elemental and crystalline distributions ($1.5 \times 1.5 \mu\text{m}$ step size for a $1.5 \times 3.0 \mu\text{m}$ beam size) in a calcined $\text{Mg}_{70.0}\text{Al}_{30.0}$ strut (state C). Horizontal: $90 \mu\text{m}$ ($1.5 \mu\text{m}$ steps); Vertical: $50 \mu\text{m}$ ($1.5 \mu\text{m}$ steps); Time: 1 s per point. The unidentified 1.397\AA Bragg peak might be attributed to the most intense reflection (044) of $\gamma\text{-Al}_2\text{O}_3$.



Mg-Al spinel with Al-Rh substitution
and without inversion:



$\text{Mg}(\text{Rh}_x\text{Al}_{1-x})_2\text{O}_4$:

$x = 70\%$,
 $a = 8.4107\text{\AA}$,
 $u = 0.3901$

MgAl_2O_4 :

$x = 0\%$,
 $a = 8.0855\text{\AA}$,
 $u = 0.3901$

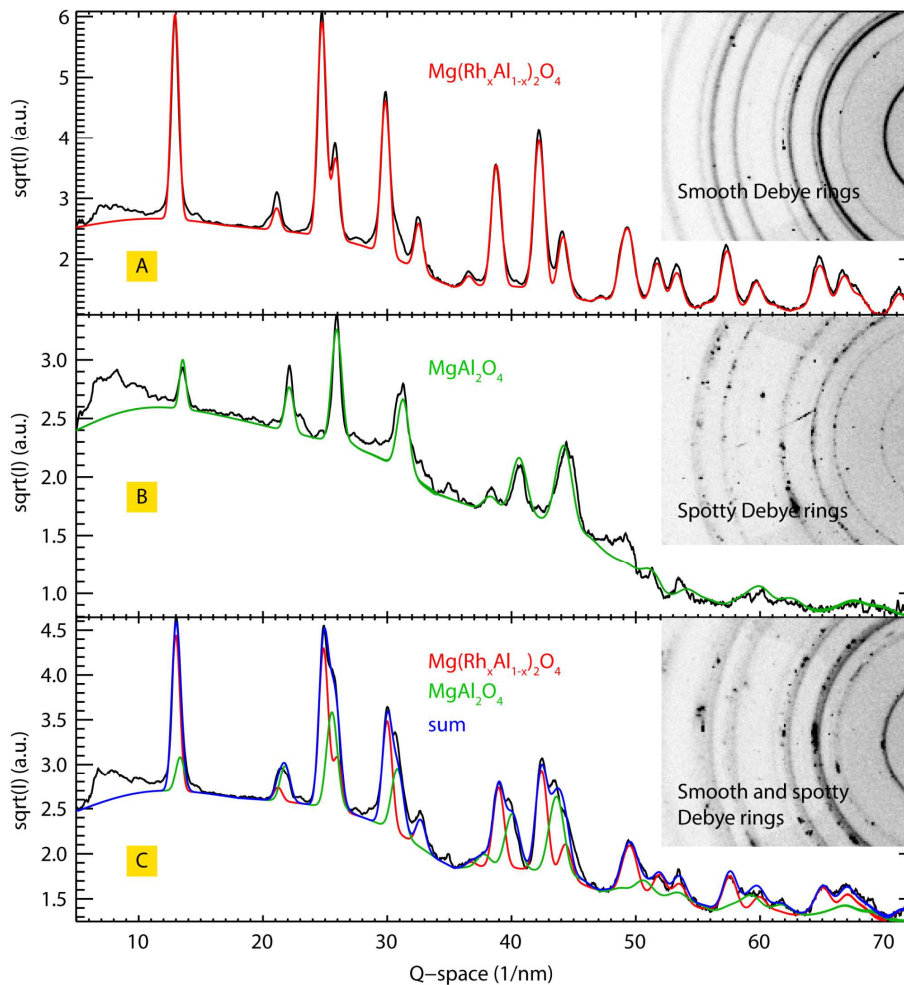


Figure S4. Diffractograms of $\text{Mg}(\text{Rh}_x\text{Al}_{1-x})_2\text{O}_4$ (A), MgAl_2O_4 (B) and of a mixture of the two (C) selected from a tomographic scan of $\text{Rh}_{13.6}\text{Mg}_{86.4}$ (state C). Translation: $190\ \mu\text{m}$ ($1.5\ \mu\text{m}$ steps); Rotation: 180° (1.2° steps); Time: 1 s per point. Not only the lattice parameter (and hence Bragg peak shifts) and atomic substitution (and hence Bragg peak intensities) allow for a distinction, but also the appearance of the Debye rings (smooth or spotty) and the peak intensity ratios.

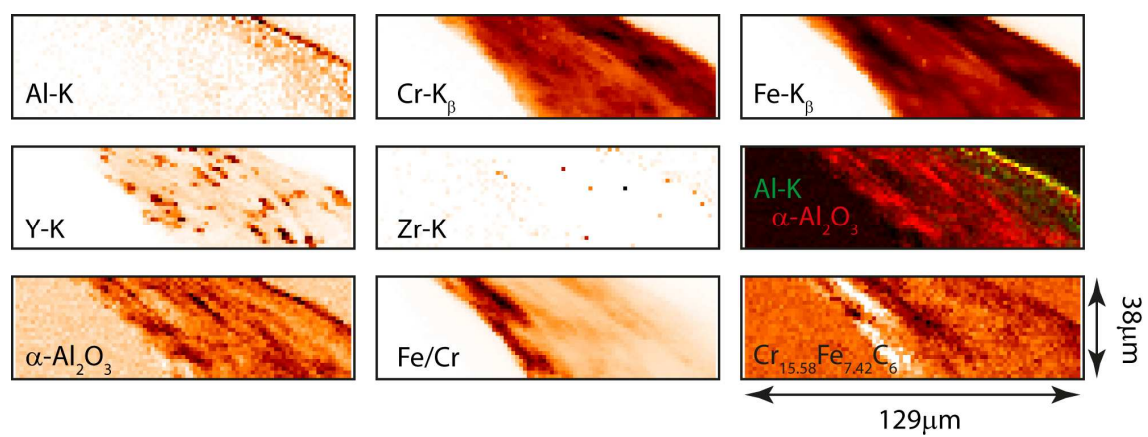


Figure S5. Projected elemental and crystalline distributions in calcined bare foam strut.

Horizontal: 129 μm (1.5 μm steps); Vertical: 38 μm (1.5 μm steps); Time: 1 s per point.

μ XRF/XANES.

Rhodium speciation by XANES.

The applied energy step size was adapted to slope at different energies in the XANES spectrum, meaning that the smallest step size is chosen around the Rh-L₃ edge (2920 eV - 2954 eV: 2 eV, 2955 eV - 2980 eV: 1 eV, 2980.5 eV - 3000 eV: 0.5 eV, 3000.25 eV - 3014 eV: 0.25 eV, 3014.5 eV - 3075 eV: 0.5 eV and 3076 eV - 3135 eV: 1 eV). A 1.6 s acquisition time was employed for each energy, resulting in ~ 14 min recording time for one spectrum. Several repeats with a maximum of 3 were recorded for each measured point in order to reduce noise.

Rh-L₃ spectra typically show a white-line in the range of 3005-3007 eV (depending on the oxidation state) due to the electron transition from 2p_{3/2} to 4d_{3/2} and 4d_{5/2}¹ whose intensity is known to be correlated with the number of 4d-holes.² A decrease of the white-line intensity is thus observed in the more reduced samples.³ Peaks at energies above the white-line are attributed to transitions to pd, df, f and df orbitals.¹ Since linear combination fitting (LCF) of unknown sample spectra with reference spectra is used to determine the Rh speciation, nine reference compounds were measured. Three compounds in which Rh is present in a spinel-type phase: calcined RhMgAlO₄, Rh₁₁Mg₇₀Al₁₉ and Rh₅Mg₇₀Al₂₅, two hydroxide compounds (starting products): Rh₁₁Al₈₉ and Rh₁₁Mg₇₀Al₁₉ (hydrotalcite), Rh metal, Rh₂O₃ (as received and calcined at 900°C) and calcined MgRh₂O₄ were measured. All measured reference spectra were corrected for self-absorption using the built-in function of ATHENA, influencing only the intensity of the white line. Some reference spectra, however, did not show significant differences relative to others: all three Rh spinel compounds, both hydroxide compounds and both Rh₂O₃ compounds essentially show an identical XANES spectrum, reducing the number of reference spectra to five. PCA analysis of all sample spectra discussed in this article revealed that 3 components are needed to sufficiently reconstruct all unknown XANES

spectra. Interestingly, none of the combinations of the described five spectra resulted in satisfactory LCF for all measured samples. However, when including a spectrum of the coated foam after CPO tests into the fitting model (state E), together with calcined $\text{Rh}_{5.0}\text{Mg}_{70.0}\text{Al}_{25.0}$ (state C, presence determined by XRPD analysis) and Rh_2O_3 (reference compound, presence determined by TPR), it was possible to adequately describe all other sample spectra.

Table S1. Summary of the Rh speciation of all measured samples determined by means of linear combination fitting of unknown spectra with three reference spectra: $\text{Rh}_{5.0}\text{Mg}_{70.0}\text{Al}_{25.0}$ spinel, Rh_2O_3 and a spectrum of a $\text{Rh}_{11.0}\text{Mg}_{70.0}\text{Al}_{19.0}$ strut (state E). The percentages represent the amount of Rh present as each given reference compound. Since spectrum 5c_1 is used as a reference to fit all other spectra no results can be given for this spectrum.

Sample		SA dRh _{5.0} Mg _{70.0} Al _{25.0}	Sample5c_1	SA dRh ₂ O ₃
Rh _{11.0} Mg _{70.0} Al _{19.0} _State C_1	5a_1	0.41	0.60	0.00
Rh _{11.0} Mg _{70.0} Al _{19.0} _State C_2	5a_2	0.30	0.68	0.02
Rh _{11.0} Mg _{70.0} Al _{19.0} _State C_3	5a_3	0.62	0.28	0.10
Rh _{11.0} Mg _{70.0} Al _{19.0} _State C_4	5a_4	0.25	0.75	0.00
Rh _{11.0} Mg _{70.0} Al _{19.0} _State C_5	5a_5	0.49	0.51	0.00
Rh _{11.0} Mg _{70.0} Al _{19.0} _State C_6	5a_6	0.09	0.91	0.00
Rh _{11.0} Mg _{70.0} Al _{19.0} _State C_7	5a_7	0.37	0.43	0.19
Rh _{11.0} Mg _{70.0} Al _{19.0} _State C_8	5a_8	0.36	0.32	0.32
Rh _{11.0} Mg _{70.0} Al _{19.0} _State C_9	5a_9	0.23	0.64	0.13
Rh _{11.0} Mg _{70.0} Al _{19.0} _State C_10	5a_10	0.27	0.44	0.30
Rh _{11.0} Mg _{70.0} Al _{19.0} _State C	5a_11	0.32	0.50	0.18
Rh _{11.0} Mg _{70.0} Al _{19.0} _State D_1		0.19	0.81	0.00
Rh _{11.0} Mg _{70.0} Al _{19.0} _State D_2		0.06	0.94	0.00
Rh _{11.0} Mg _{70.0} Al _{19.0} _State D_3		0.13	0.86	0.00
Rh _{11.0} Mg _{70.0} Al _{19.0} _State D_4	5b_1	0.11	0.89	0.00
Rh _{11.0} Mg _{70.0} Al _{19.0} _State D_5	5b_2	0.17	0.83	0.00
Rh _{11.0} Mg _{70.0} Al _{19.0} _State D_6		0.39	0.61	0.00
Rh _{11.0} Mg _{70.0} Al _{19.0} _State D_7		0.32	0.65	0.04
Rh _{11.0} Mg _{70.0} Al _{19.0} _State D_8		0.22	0.78	0.00
Rh _{11.0} Mg _{70.0} Al _{19.0} _State D_9		0.15	0.85	0.00
Rh _{11.0} Mg _{70.0} Al _{19.0} _State D_10		0.20	0.80	0.00
Rh _{11.0} Mg _{70.0} Al _{19.0} _State E_1		0.27	0.70	0.03
Rh _{11.0} Mg _{70.0} Al _{19.0} _State E_2		0.06	0.94	0.00
Rh _{11.0} Mg _{70.0} Al _{19.0} _State E_3		0.14	0.85	0.01
Rh _{11.0} Mg _{70.0} Al _{19.0} _State E_4		0.00	1.00	0.00
Rh _{11.0} Mg _{70.0} Al _{19.0} _State E_5	5c_1	n.a.	n.a.	n.a.
Rh _{11.0} Mg _{70.0} Al _{19.0} _State E_6	5c_2	0.00	1.00	0.00
Rh _{11.0} Mg _{70.0} Al _{19.0} _State E_7	5c_3	0.00	1.00	0.00
Rh _{11.0} Mg _{70.0} Al _{19.0} _State E_8	5c_4	0.00	1.00	0.00
Rh _{13.6} Mg _{86.4} _State C_1		0.39	0.61	0.00
Rh _{13.6} Mg _{86.4} _State C_2		0.28	0.56	0.16
Rh _{13.6} Mg _{86.4} _State C_3		0.76	0.24	0.00
Rh _{13.6} Mg _{86.4} _State C_4		0.64	0.36	0.00
Rh _{13.6} Mg _{86.4} _State C_5		0.88	0.12	0.00

REFERENCES

- (1) Sham, T. K. *Phys. Rev. B* **1985**, *31*, 1888–1902.
- (2) de Groot, F. M. F.; Hu, Z. W.; Lopez, M. F.; Kaindl, G.; Guillot, F.; Trone, M. J. *Chem. Phys.* **1994**, *101*, 6570–6576.
- (3) Shimizu, K.-i.; Oda, T.; Sakamoto, Y.; Kamiya, Y.; Yoshida, H.; Satsuma, A. *Appl. Catal. B: Env.* **2012**, *111–112*, 509–514.